WIND ENERGY
Wind Energ. 0000; **00**:1–17
DOI: 10.1002/we

RESEARCH ARTICLE

Development of a 5 MW Reference Gearbox for Offshore Wind Turbines

Amir Rasekhi Nejad[1,2], Yi Guo[3], Zhen Gao[2] and Torgeir Moan[1,2]

[1]Norwegian Research Center for Offshore Wind Technology (Nowitech), Norwegian University of Science and Technology (NTNU)
[2]Center for Ships and Ocean Structures (CeSOS), Norwegian University of Science and Technology (NTNU)
[3]National Wind Technology Center (NWTC), National Renewable Energy Laboratory (NREL), USA

ABSTRACT

This paper presents detailed descriptions, modelling parameters and technical data of a 5 MW high speed gearbox developed for the National Renewable Energy Laboratory (NREL) offshore 5 MW baseline wind turbine. The main aim of this article is to support the concept studies and researches for large offshore wind turbines by providing a baseline gearbox model with detailed modelling parameters. This baseline gearbox follows the most conventional design types of those used in wind turbines. The gearbox consists of three stages, two planetary and one parallel stage gears. The gear ratios among the stages are calculated in a way to obtain the minimum gearbox weight. The gearbox components are designed and selected based on the offshore wind turbine design codes and validated by comparison with the data available from the manufacturer of large offshore wind turbine prototypes. All parameters required to establish the dynamic model of the gearbox are then provided. Moreover, a maintenance map indicating components with high to low probability of failure is shown. The 5 MW reference gearbox can be used as a baseline for research on wind turbine gearboxes and comparison studies. It can also be employed in global analysis tools to represent a more realistic model of gearbox in the coupled analysis. Copyright © 0000 John Wiley & Sons, Ltd.

KEYWORDS

5 MW Reference Gearbox, Offshore Wind Turbines, High Speed Wind Turbine Gearbox, Wind Turbine Drivetrain

Correspondence

Center for Ships and Ocean Structures (CeSOS), Norwegian University of Science and Technology (NTNU), NO-7491, Trondheim, Norway. E-mail: Amir.Nejad@ntnu.no

Received . . .

1. INTRODUCTION

The wind energy industry has been in fast development track over last decade particularly in offshore fields, because of high and steady winds over sea waters. In offshore wind farms, the industry trend is toward multi megawatts, large wind turbines to harvest more energy from every turbine. For instance, the annual electricity production of one single 5 MW wind turbine is enough for 1250 homes in USA [1]. While many conceptual studies are devoted to upscale the structural components (e.g. blades, tower and nacelle) and to investigate the dynamic load and load response in larger wind turbines components, (e.g. [1]-[2]), the drivetrains and in particular gearboxes, appear to be overlooked. Gears are yet the dominant technology in wind turbine drivetrains, with the market share above 85% [3], both onshore and offshore. In offshore development and in large turbines, the models such as Vestas 3.3 MW [4], REpower 5 MW [5] or Areva 5 MW [6] are fitted with gearboxes. In research and development side, however, there is a lack of a reference, baseline gearbox design for analysis and comparison of different turbine concepts. Many researches have used the publicly available gearbox from Gearbox Reliability Collaborative (GRC) at National Renewable Energy Laboratory (NREL). The NREL GRC 750 kW gearbox [7] has been used in various studies on fixed offshore [8],[9],[10],[11] or on a floating wind turbine[12]. However, as the industry goes offshore with higher capacity, there is a need for a baseline gearbox design with adequate modelling parameters for multi megawatts turbines to support the research studies. The challenges in large offshore wind turbines should be well studied by detailed modelling and simulations to avoid costly problems during operations.

The objective of this paper is to establish detailed specifications of a gearbox representing the typical gearboxes suitable for large offshore wind turbines. All modelling parameters are provided; thus, one can replicate the gearbox model. In practice, apart from the minimum requirements set by design codes, many project-specific factors such as site condition, installation issues, weight, manufacturing limitation and material availability influence the gearbox design. In this paper, a system engineering design approach has been employed. At first, the gear speed ratios are calculated by DriveSE model - a tool for minimizing the gearbox weight in wind turbines. By having the optimized gear speed ratios, the gearbox components are then designed and selected.

The reference gearbox in this paper is designed for the NREL offshore 5 MW baseline wind turbine [1] on a bottom-fixed structure in the North sea.

2. DESIGN BASIS & METHODOLOGY

2.1. Wind Turbine Specification

In this study, the NREL offshore 5 MW baseline wind turbine [1] installed on a bottom-fixed offshore structure is considered. The NREL 5 MW turbine is a three blades, upwind, pitch controlled turbine with specification presented in Table I. The turbine class is selected as IEC class B according to IEC 61400-1 [13].

Table I. NREL 5 MW Wind Turbine Specification [1].

Parameter	Value
Type	Upwind/3 Blades
Rated power (MW)	5
Cut-in wind speed (m/sec)	3
Cut-out wind speed (m/sec)	25
Rated wind speed (m/sec)	11.4
Rated rotor speed (rpm)	12.1
Hub height, above mean sea level (m)	90
Rotor diameter (m)	126
Hub diameter (m)	3
Rotor mass ($\times$1000 kg)	110
Tower mass ($\times$1000 kg)	347.5
Nacelle mass ($\times$1000 kg)	240
Hub mass ($\times$1000 kg)	56.8
Power control system	Pitch/Constant Power

2.2. Environmental Condition

The wind turbine installation site is considered to be an offshore field in the Northern side of North sea. Since the wind turbine is bottom-fixed, the influence of wave loads on the drivetrain response can be neglected. The probability density function of one hour mean wind speed, u, at 10 m above the average sea level is modelled by the 2-parameters Weibull distribution [14],[15]:

$$F_U(u) = 1 - exp(-(\frac{u}{a})^c) \tag{1}$$

DOI: 10.1002/we
Prepared using weauth.cls

in which a and c are the shape and scale parameters which are 8.426 and 1.708 for Northern North sea respectively [14]. The wind speed at hub height is calculated by power law, with power value of 0.14 for offshore as [16]:

$$u_{hub} = u(\frac{h_{hub}}{10})^{0.14} \tag{2}$$

where h_{hub} is the hub height. The cut-in, rated and cut-out wind speeds in the wind turbine specifications refer to the wind speed at the nacelle height [13], which is 90 m above the average sea level for this case study turbine.

2.3. Global Load and Load Response Analysis

A decoupled analysis method is used to estimate the drivetrain dynamic load response from the environmental load - see Fig. 1.

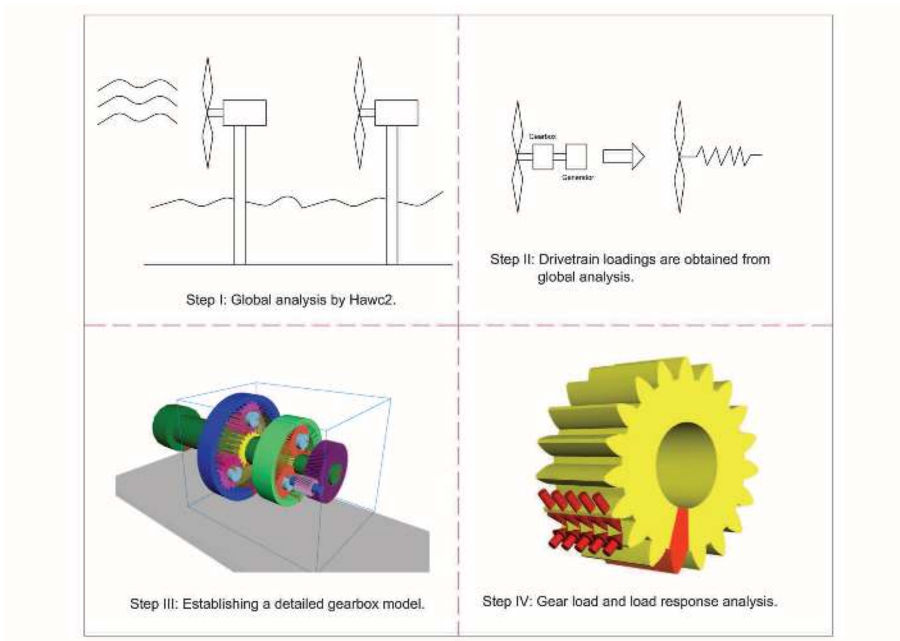

Figure 1. Decoupled approach for wind turbine gearbox analysis.

The global analysis is conducted by using the aero-servo-elastic code HAWC2 [17]. Simulations are carried in operational conditions and from cut-in to cut-out wind speeds. To minimize the statistical uncertainties, 15 simulations are carried out for each wind speed over 800 sec. and the first 200 sec. is removed to avoid start-up transient effects. The reference turbulence intensity factor is taken as 0.14 for all the wind speeds, according to IEC 61400-1 class B turbine [13]. The transit load cases, such as emergency shutdown or fault conditions are evaluated in a companion paper [18].

More information about decoupled approach and its limitations can be found in Nejad et al. [19],[20], [21] or Dong et al. [8].

2.4. System Engineering Design Approach

Gearbox is a part of the wind turbine system which its type and design influences other parts like tower and nacelle. Therefore, a system engineering approach should be consulted. In this study, the rest of the turbine configuration is fixed and so the sizing of the gearbox is self-contained. From a full system perspective, the gearbox design impacts and is impacted by the rotor and rest of drivetrain design. Given the relative expense of the gearbox relative to other system components, trade-offs in the design may lead to an even lower weight gearbox in a full turbine design optimization.

The System Engineering Project at National Renewable Energy Laboratory developed the DriveSE model. This model performs drivetrain sizing and cost analysis for the minimum weight and its results compare well with industry data. DriveSE consists of a series of interacting mathematical models of drivetrain components, including the hub, low speed shaft, main bearings, the gearbox, bedplate, generator, and yaw systems. The generator and the rest of drivetrain components are sized based on empirical data. DriveSE interfaces with other wind turbine components, namely, the rotor and tower. At this top level, design criteria on allowable stress and deflection are inherently included for individual drivetrain subcomponents. These design criteria, together with the minimum weight objective for sub-optimizations, are used to determine the subcomponent dimensions. Key model inputs include the extreme aerodynamic rotor loads (torque and non-torque), gravity loads, gearbox configurations, and design parameters such as rotor overhang and gearbox location. A fatigue analysis of the low speed shaft and main bearing(s) is included with several additional inputs. The outputs fall into two categories: subcomponent outputs and system outputs. Subcomponent outputs include the dimension and weight of individual subcomponents, and gearbox stage ratio and stage volume, which are preliminary design parameters for these subcomponents. The mass outputs for all the individual components are then used in a turbine cost model as part of overall system cost analysis. The system outputs are the cumulative weight, moments of inertia, and center of gravity of the entire hub and nacelle assemblies, which are used as inputs at the tower design level.

More information about the gearbox design as part of the overall wind turbine design process can be found in Dykes et al. [22], [23].

2.4.1. Optimizing Gear Stage Speed Ratios for Minimizing Gearbox Weight

In this paper, the NREL DriveSE software has been used to minimize the gearbox weight. The DriveSE tool designs the gearboxes for the minimum weight by optimizing the stage speed ratio [24, 25, 26, 27, 28]. The model requires the minimum input: transmitted torque, overall speed ratio, stage number, and gearbox configuration. The gearbox model outputs the weight, volume, and speed ratio of gearbox stages. These parameters are crucial input for gearbox component design and drivetrain capital/OEM cost analyses. This model is established based on ISO/AGMA gearbox design standards [24, 25, 26, 27, 28]. Input torque has been the major design driver of wind turbine gearboxes. Influences of non-torque loads caused by rotor overhung weight and aerodynamic forces on gearbox weight are considered in this work by including various main shaft/bearing configurations. The gearbox rating (bending and pitting resistance) analysis is not the focus of this approach so that the resulting changes to the gearbox design are not included. This model is validated by actual gearbox weight and speed ratios for wind turbines with power ratings between $750\,kW$ and $5MW$, which are specified by gearbox manufacturers. Figure 2 shows the validation results.

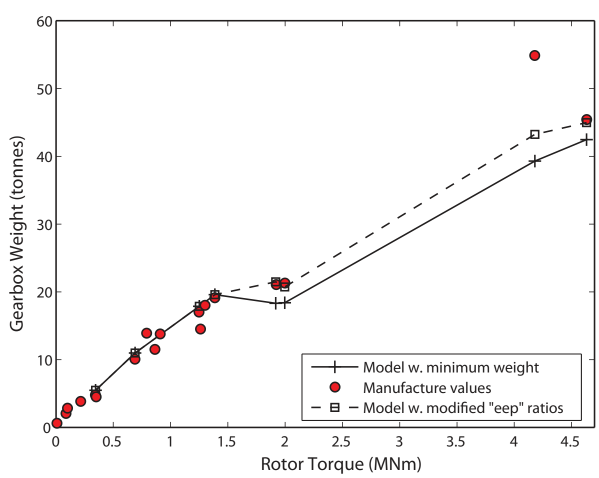

Figure 2. Validation of DriveSE weight minimizing tool.

Wind Energ. 0000; **00**:1–17 © 0000 John Wiley & Sons, Ltd.
DOI: 10.1002/we
Prepared using weauth.cls

(a) An external gear pair

The relationship between the overall gear dimensions, the speed ratio U_s, and power P for external gears is [29]:

$$C^2F = \frac{31,500P(U_s+1)^3}{Kn_pU_s} \tag{3}$$

where $C = 0.5d_p(U_s+1)$ is the center distance. d_p and F are the gear diameter and facewidth. The transmitted power $P = \frac{Tn_p}{63,000}$ is linearly correlated to the gearbox torque T and speed n_p. K factor is an index for measuring the intensity of tooth loads [29]. There are different ways to calculate K factor: 1). it can be estimated from the empirical table in [29](2.45); 2). it can be calculated by the formula below when the gearbox component dimensions are designed. In the study, the first approach is used:

$$K = \frac{W_t}{Fd}\frac{U_s+1}{U_s} \tag{4}$$

where $W_t = \frac{2Q_p}{d_p}$ is the tangential driving force. Q_p is the input torque to the pinion.

Rewriting Eq. 3:

$$Fd_p^2 = \frac{2Q_p}{K}\frac{U_s+1}{U_s} \tag{5}$$

The gearbox weight is estimated by $W_{GB} = K_{AG}Fd_p^2$, where K_{AG} is the application factors for weight estimations [30]. The final form is:

$$W_{GB} = K_{AG}\frac{2Q_p}{K}\frac{U_s+1}{U_s} \tag{6}$$

The volume of driving gear equals Fd_p^2. The driven gear volume is $Fd_p^2U_s^2$. Therefore, the total size of the gear pair equals:

$$\sum Fd^2 = Fd_p^2 + Fd_g^2 = Fd_p^2 + Fd_p^2U_s^2 \tag{7}$$

The total weight of the gear pair equals:

$$\begin{aligned} W_{GBPN} &= K_{AG}\tfrac{2Q_p}{K}(\tfrac{U_s+1}{U_s}) + K_{AG}\tfrac{2Q_p}{K}(\tfrac{U_s+1}{U_s})U_s^2 \\ &= K_{AG}\tfrac{2Q_p}{K}(1+\tfrac{1}{U_s}+U_s+U_s^2) \end{aligned} \tag{8}$$

(b) Planetary gear stage

The volume of a planetary gear consists of the sun, ring, and B planet gears. The sun gear volume is:

$$Fd_s^2 = \frac{2Q_s}{BK}(\frac{U_{SN}+1}{U_{SN}}) \tag{9}$$

where $u_{SN} = 0.5U_s - 1$ is the speed ratio between the sun and planet. Q_s is the input torque to the sun gear.

The volume of a planet is:

$$Fd_p^2 = Fd_s^2U_{SN}^2 = \frac{2Q_s}{BK}(\frac{U_{SN}+1}{U_{SN}})U_{SN}^2 \tag{10}$$

The volume of the ring gear depends on both its diameter and thickness. AGMA 6123 defines the ring thickness no less than 3 times module. The ring gear volume is approximated empirically without designing individual gear dimensions. The ring volume considers the weight of the housing and carrier:

$$V_r = K_rFd_s^2(\frac{d_r}{d_s})^2 = K_r\frac{2Q_s}{BK}(\frac{U_{SN}+1}{U_{SN}})(\frac{d_r}{d_s})^2 \tag{11}$$

where $K_r = 0.4$ is the scaling factor, selected from [30].

Therefore, the overall planetary gear volume is:

$$\begin{aligned} Fd_s^2 + BFd_p^2 + V_r &= \tfrac{2Q_s}{BK}(\tfrac{U_{SN}+1}{U_{SN}}) + B\tfrac{2Q_s}{BK}(\tfrac{U_{SN}+1}{U_{SN}})U_{SN}^2 + K_r\tfrac{2Q_s}{BK}(\tfrac{U_{SN}+1}{U_{SN}})(\tfrac{d_r}{d_s})^2 \\ &= \tfrac{2Q_s}{BK}[\tfrac{1}{B} + \tfrac{1}{BU_{SN}} + U_{SN} + U_{SN}^2 + K_r\tfrac{(U_s-1)^2}{B} + K_r\tfrac{(U_s-1)^2}{BU_s}] \end{aligned} \tag{12}$$

The planetary gear weight equals:

$$W_{GSEN} = K_{AG}\frac{2Q_s}{K}[\frac{1}{B} + \frac{1}{BU_{SN}} + U_{SN} + U_{SN}^2 + K_r\frac{(U_s-1)^2}{B} + K_r\frac{(U_s-1)^2}{BU_{SN}}] \tag{13}$$

(c) Gearbox Weight

The gearbox weight is the summation of individual stage weight, which depends on the input torque Q_1, Q_1, Q_3 and speed ratio U_1, U_2, U_3. For the 5 MW reference gearbox with planetary-planetary-parallel configuration, the total weight is:

$$W_{GB} = W_{GSEN}^1 + W_{GSEN}^2 + W_{GBPN}^3 \tag{14}$$

The final gearbox design takes into account of gear dynamic effects on loads, overload, unequal load sharing for planetary gears, and main shaft configuration. Therefore, the gearbox weight - W_{GB}^0, equation 15 - considers overload factor K_0 [31], dynamic factor K_v [24], load sharing factor among planets $K_{\gamma p}$ [28], load sharing factors between rows $K_{\gamma b}$ (from GRC test data, new design parameter proposed to AGMA standard committee), and a new factor that captures the effects of main shaft configurations on gearbox loads K_{SH}. In the model, $k_{SH} = 1$ is used as default. More gearbox design information will be gathered to determine its appropriate value.

$$W_{GB}^0 = K_0 K_v K_{\gamma p} K_{\gamma b} K_{SH} W_{GB} \tag{15}$$

2.4.2. Determination of gearbox speed ratio per stage

This method selects the optimal speed ratios of individual gear stages for minimizing gearbox weight. For the configuration of Planetary-Planetary-Parallel, the total volume of the gearbox equals:

$$\begin{aligned} V = \; & \tfrac{2Q_0}{K}\tfrac{1}{U_1}\left[\tfrac{1}{B_1} + \tfrac{1}{B_1(\frac{U_1}{2}-1)} + (\tfrac{U_1}{2}-1) + (\tfrac{U_1}{2}-1)^2 + K_{r1}\tfrac{(U_1-1)^2}{B_1} + K_{r1}\tfrac{(U_1-1)^2}{B_1(\frac{U_1}{2}-1)}\right] \\ & + \tfrac{2Q_0}{K}\tfrac{1}{U_1U_2}\left[\tfrac{1}{B_2} + \tfrac{1}{B_2(\frac{U_2}{2}-1)} + (\tfrac{U_2}{2}-1) + (\tfrac{U_2}{2}-1)^2 + K_{r2}\tfrac{(U_2-1)^2}{B_2} + K_{r2}\tfrac{(U_2-1)^2}{B_2(\frac{U_2}{2}-1)}\right] \\ & + \tfrac{2Q_0}{K}\tfrac{1}{U_1U_2U_3}\left[1 + \tfrac{1}{U_3} + U_3 + U_3^2\right] \end{aligned} \tag{16}$$

where Q_0 is main shaft input torque. Let $M_1 = U_1U_2$, $M_2 = U_2U_3$, and $M_0 = U_1U_2U_3$ and rewrite Eq. 16 as:

$$\begin{aligned} V(M_1, U_1) = \; & \tfrac{2Q_0}{K}\tfrac{1}{U_1}\left[\tfrac{1}{B_1} + \tfrac{1}{B_1(\frac{U_1}{2}-1)} + (\tfrac{U_1}{2}-1) + (\tfrac{U_1}{2}-1)^2 + K_{r1}\tfrac{(U_1-1)^2}{B_1} + K_{r1}\tfrac{(U_1-1)^2}{B_1(\frac{U_1}{2}-1)}\right] \\ & + \tfrac{2Q_0}{K}\tfrac{1}{M_1}\left[\tfrac{1}{B_2} + \tfrac{1}{B_2(\frac{M_1}{2U_1}-1)} + (\tfrac{M_1}{2U_1}-1) + (\tfrac{M_1}{2U_1}-1)^2 + K_{r2}\tfrac{(\frac{M_1}{U_1}-1)^2}{B_2} + K_{r2}\tfrac{(\frac{M_1}{U_1}-1)^2}{B_2(\frac{M_1}{2U_1}-1)}\right] \\ & + \tfrac{2Q_0}{K}\tfrac{1}{M_0}\left[1 + \tfrac{M_1}{M_0} + \tfrac{M_0}{M_1} + (\tfrac{M_0}{M_1})^2\right] \end{aligned} \tag{17}$$

$$\begin{aligned} V(M_2, U_2) = \; & \tfrac{2Q_0}{K}\tfrac{M_2}{M_0}\left[\tfrac{1}{B_1} + \tfrac{1}{B_1(\frac{M_0}{2M_2}-1)} + (\tfrac{M_0}{2M_2}-1) + (\tfrac{M_0}{2M_2}-1)^2 + K_{r1}\tfrac{(\frac{M_0}{M_2}-1)^2}{B_1} + K_{r1}\tfrac{(\frac{M_0}{M_2}-1)^2}{B_1(\frac{M_0}{2M_2}-1)}\right] \\ & + \tfrac{2Q_0}{K}\tfrac{M_2}{M_0U_2}\left[\tfrac{1}{B_2} + \tfrac{1}{B_2(\frac{U_2}{2}-1)} + (\tfrac{U_2}{2}-1) + (\tfrac{U_2}{2}-1)^2 + K_{r2}\tfrac{(U_2-1)^2}{B_2} + K_{r2}\tfrac{(U_2-1)^2}{B_2(\frac{U_2}{2}-1)}\right] \\ & + \tfrac{2Q_0}{K}\tfrac{1}{M_0}\left[1 + \tfrac{U_2}{M_2} + \tfrac{M_2}{U_2} + (\tfrac{M_2}{U_2})^2\right] \end{aligned} \tag{18}$$

DOI: 10.1002/we

$$\begin{aligned}\frac{dV(M_1,U_1)}{dU_1} = \quad & -\frac{(U_1-1)(1+K_r(U_1-1)^2)}{B_1U_1^2(\frac{U_1}{2}-1)^2} + \frac{2K_r(U_1-1)}{B_1U_1(\frac{U_1}{2}-1)} - \frac{(1+K_r)}{B_1U_1^2} + \frac{1}{4} + \frac{K_r}{B_1} + \frac{1}{2B_2(\frac{M_1}{2}-U_1)^2} \\ & -\frac{2K_r(M_1-U_1)}{B_2U_1^2(\frac{M_1}{2}-U_1)} + \frac{K_r(M_1-U_1)^2}{2B_2U_1^2(\frac{M_1}{2}-U_1)^2} + (\frac{1}{2} + \frac{2K_r}{B_2})(\frac{1}{U_1^2} - \frac{M_1}{U_1^3})\end{aligned} \tag{19}$$

$$\begin{aligned}\frac{dV(M_2,U_2)}{dU_2} = \quad & -\frac{M_2(U_2-1)(1+K_rM_2(U_2-1)^2)}{M_0B_2U_2^2(\frac{U_2}{2}-1)^2} + \frac{2K_rM_2(U_2-1)}{M0B_2U_2(\frac{U_2}{2}-1)} \\ & +(\frac{M_2}{4M_0} + \frac{K_rM}{M_0B_2} + \frac{1}{M_2M_0}) + \frac{(-\frac{M_2}{M_0B_2} - \frac{K_rM}{M0B_2} - \frac{M_2}{M_0})}{U_2^2} - \frac{2M^2}{M_0U_2^3}\end{aligned} \tag{20}$$

$\frac{dV(M_1,U_1)}{dU_1}$, $\frac{dV(M_1,U_1)}{dU_1}$ can also calculated numerically by using finite differences. Central difference formulation $\frac{dV(U+dU)-dV(U-dU)}{2dU}$ (second order accuracy) is used here to check the accuracy of the analytical formulations in Eqs 19 and 20. $dU = 2 \times 10^{-5}$ is selected through a sensitivity test to find the optimal step size to avoid machine round off.

Global Newton iteration is used to find the roots of Eq. 19 and Eq. 20: U_1 and U_2 for a given $M_1 = U_1U_2$. The iteration procedure is based on the [32]. The general procedure is described as below:

1. Select an initial value for $M_1 = U_1U_2$
2. Set the derivative of the gearbox volume to zero. $\frac{dV_{GB}}{dU_1} = 0$
3. Solve for the root U_1
4. $U_2 = M_1/U_1$
5. $U_3 = M_0/M_1$, where M_0 is total gear ratio
6. $M_2 = U_2U_3$
7. Solve for U_2 from $\frac{dV_{GB}}{dU_2} = 0$
8. Iterate until U_2 from step 7 equals U_2 from step 4.

Convergence tolerance used in the iteration is 5×10^{-3}.

2.5. Gearbox Type and Component Design

Today, many gearbox designs including high speed [4],[5], medium speed [6], variable speed [33] or multiple shafts [34] have been offered by the wind turbine suppliers and gearbox manufacturers. Among the gearbox designs available in the market, the high speed gearbox with gear ratio in the range of 1:80-1:120 is the most common design. The Vestas offshore products including Vestas V112-3.3 [4] use high speed gearboxes, with two planetary and one parallel stage. The REpower 5 MW turbine [5] has employed the similar high speed gearbox with three stages.

For the 5 MW reference gearbox, the most common high speed gearbox with two planetary stage and one parallel stage is selected. For offshore applications, the use of spur gears is also possible since the noise is not a primary concern. Spur gears are easy to manufacture and perform best at low speed and high torques. The disadvantage of employing spur gears is noise, particularly in high speed applications, which can be reduced by gear lead and profile modifications. In the first and second stages of this reference gearbox, spur gears are used in planetary configurations. Moreover, spur gears do not generate axial or trust load. This can have a positive impact on the planet bearings which are the most vulnerable components in planetary gears [10]. The gears in the high speed stage are selected as parallel helical gears.

The gear ratio of each stage is selected in a way to minimize the total gearbox weight as described in the last section, 2.4. Table II shows the design options calculated by the weight minimizing tool. Option B with three planets for both planetary stages is selected. Option C or D were not chosen as the gain in weight does not justify the complexities added to the load sharing behaviour in four planets design [35].

The gearbox components, e.g. gears, bearings and shafts are designed based on the loads obtained from the global analysis and following the offshore wind turbine gearbox design code, IEC 61400-4 [28]. Components are designed to withstand the fatigue damage and ultimate loads during normal operational conditions. The ultimate operational loads on the gearbox is taken from an earlier study [20] for the same offshore site. The gear fatigue damage is also calculated by a long-term approach considering the whole range of operational conditions [19]. The gears are designed based on the ISO

DOI: 10.1002/we
Prepared using weauth.cls

Table II. Gearbox speed ratio options.

	A	B	C	D
1^{st} stage	1:5.1944 (3p)	1:3.9549 (3p)	1:3.8322 (4p)	1:3.9502 (3p)
2^{nd} stage	1:6.2247 (3p)	1:6.1695 (3p)	1:6.2367 (3p)	1:6.1262 (4p)
3^{rd} stage	1:3.0000	1:3.9754	1:4.0586	1:4.0083
Total dry weight ($\times$1000 kg)	53.69	48.82	43.98	47.30

p=planets

6336-2 [25], ISO 6336-3 [27] and ISO 6336-6 [36] and with the load and safety factors recommended by IEC 61400-4 [28]. The KISSsoft 2014 [37] was used for initial gear sizing.

The bearings types are selected based on IEC 61400-4 [28] recommendation, 750 kW NREL gearbox design [7] and REpower 5 MW [38]. The main shaft is supported by two main bearings to minimise non-torque loadings on the gearbox.

The effect of transient loads, i.e. emergency shutdown or fault conditions on the gearbox is investigated in a separate work [18] by using a detailed multibody model (MBS) of this reference gearbox - see section 2.6 for the MBS model.

2.6. Gearbox Multibody System (MBS) Model

The multibody system (MBS) modelling is a powerful tool for load and dynamic response analysis of wind turbine gearboxes [8], [12], [39]. The objectives of the gearbox dynamic analysis vary from noise control to stability analysis [40]. For wind turbine gearboxes, the goals in dynamic modelling include the study of natural frequencies of the system, noise and vibration analysis, and dynamic load analysis on other components (e.g. support structure). The results from the load analysis can then be post-processed for stress analysis and life or reliability investigation.

In MBS method, a gearbox is modelled as a system of rigid or flexible bodies interconnected with appropriate joints [41], [42]. Flexible bodies - normally shafts and structural members - are first generated in a finite element software and then imported with reduced degrees of freedom in the MBS model [43], [44]. Bearings can be modelled as force elements with a linear or non-linear force-deflection relationship. Gears are modelled as rigid bodies with compliance at the teeth. A detailed modelling procedure can be find in Oyague F. [7].

The advantage of the MBS method is that dynamic effects of components are inevitably included in the analysis. Moreover non-torque forces and moments can be added to the input loadings. Nevertheless, the accuracy of the results is directly dependent on the precision of the given stiffness, inertia and damping values.

The MBS equation of motion leads in general to a form of:

$$\mathbf{M}\ddot{X} + \mathbf{C}\dot{X} + \mathbf{K}X = \mathbf{F} \tag{21}$$

where the displacement matrix **X** in a six degree of freedom (DOF) system is equal to:

$$\mathbf{X} = \begin{pmatrix} x & y & z & \alpha & \beta & \gamma \end{pmatrix}^T \tag{22}$$

The **M**, **C** and **K** are mass, damping and stiffness matrices respectively. The external force matrix **F** also includes all forces and moments:

$$\mathbf{F} = \begin{pmatrix} F_x & F_y & F_z & M_x & M_y & M_z \end{pmatrix}^T \tag{23}$$

As highlighted by Peeters et al. [44], the flexible MBS model where the rigid bodies are replaced by the reduced DOF flexible bodies, can capture the most of gearbox dynamic behaviour. However, full flexible model reduces significantly the computational time [45], thus, it should be a balance and engineering judgement on the number of DOFs which is considered in the MBS model. Table III presents the model requirements highlighted by Guo et al. [46].

DOI: 10.1002/we
Prepared using weauth.cls

The bearings in this paper are modelled with linear diagonal stiffness as:

$$\mathbf{K} = \begin{pmatrix} K_x & 0 & 0 & 0 & 0 & 0 \\ & K_y & 0 & 0 & 0 & 0 \\ & & K_z & 0 & 0 & 0 \\ & & & K_\alpha & 0 & 0 \\ & sym. & & & K_\beta & 0 \\ & & & & & K_\gamma \end{pmatrix} \tag{24}$$

The global loads, **F**, obtained from the decoupled method - see section 2.3 - are applied at the hub location in the main shaft, as shown in Fig. 5 and the generator speed is controlled on the high speed shaft. The coordinate system is also shown in Fig. 5. In this coordinate system, the K_α is zero, since α is the rotational direction.

On generator side, the generator is modelled by a proportional-integral velocity controller [12]. Let $e = \omega - \omega_{ref}$ represents the difference between angular velocity at generator shaft calculated by MBS model and reference value obtained from the global analysis. The generator torque, T_{Gen}, is then calculated from:

$$T_{Gen} = K_P e + K_I \int_0^t edt \tag{25}$$

in which K_P and K_I are proportional and integral gain receptively. The gain parameters are estimated based on the generator slip-slop diagram and to minimize the angular velocity error. In each time step, the T_{Gen} is calculated and applied on the generator shaft.

Table III. MBS model recommendation [46].

Components	Recommended modelling method
Main shaft	Flexible body
Main bearing	Stiffness matrices
Gearbox housing	Flexible body
Planetary carrier	Flexible body
Gearbox shafts	Rigid body
Gearbox support	Stiffness matrices
Gears	Rigid body
Gearbox bearings	Stiffness matrices
Spline	Stiffness matrices
Bedplate	Rigid body
Generator coupling	Stiffness matrices

In this paper, MBS model of the 5 MW reference gearbox is developed in SIMPACK [47] software. SIMPACK is a multipurpose multibody simulation code with features available to model gearboxes. The bearings are modelled with linear force-deflection relation - see equation 24. The bearing stiffness are calculated by using CalyX software, a customizable multibody dynamic finite element based contact solver engine [48] and Romax software [49].

Similar to the stiffness values, the damping in rolling element bearings is a topic with a high degree of uncertainty. Since contact damping in roller bearings is relatively small, a constant damping value can be used which is evaluated based on the average load. Kramer [50] estimated roller bearing damping by analysis of the equivalent linear spring-mass-damper system. According to Kramer [50], the roller bearing damping value varies from 0.25% to 2.5% of the stiffness. Some researchers have taken the damping equal to the 1% of the mean stiffness [51]. It should be noted that dampings should be included in MBS model for numerical reasons.

Moreover, it is important to note that gearbox is one of the elements in the wind turbine drivetrain. In a 1-DOF model of drivetrain, hub, rotor, gearbox and generator are in a series system. The equivalent inertia of such system is calculated by:

$$I_{eq} = \left(\frac{1}{I_{hub}} + \frac{1}{I_{Rotor}} + \frac{1}{I_{Gearbox}} + \frac{1}{n^2 I_{Generator}}\right)^{-1} \tag{26}$$

DOI: 10.1002/we
Prepared using weauth.cls

in which n is the inverse gearbox ratio - gearbox ratio is defined as the rotor speed over the generator speed. Similar to the inertia, the equivalent torsional stiffness of the drivetrain is obtained from:

$$K_{eq} = (\frac{1}{K_{hub}} + \frac{1}{K_{Rotor}} + \frac{1}{K_{Gearbox}} + \frac{1}{n^2 K_{Generator}})^{-1} \tag{27}$$

The frequency of free-free mode of 1 DOF drivetrain is estimated from [52]:

$$f = \frac{1}{2\pi}\sqrt{\frac{K_{eq}}{I_{eq}}} \tag{28}$$

The frequency of free-free mode of drivetrain is primary dominated by other inertias (e.g. generator and rotor) than the gearbox, but the gearbox ratio plays an important role as it increases the generator inertia significantly - see equation 26. For instance, for a high speed drivetrain design of a 2 MW wind turbine, the free-free mode frequency is about 1.36 Hz [52], while the gearbox first eigenvalue is above 5 Hz. It is the wind turbine designer responsibility to check the dynamic behaviour of whole drive line. The gearbox is an important component in drivetrain which can be used to adjust the dynamic response of the system.

3. RESULTS: 5 MW REFERENCE GEARBOX DESCRIPTION

The gearbox layout and topology with the bearing designations is shown in Figure 3 and Figure 4. The general specification is also listed in Table IV.

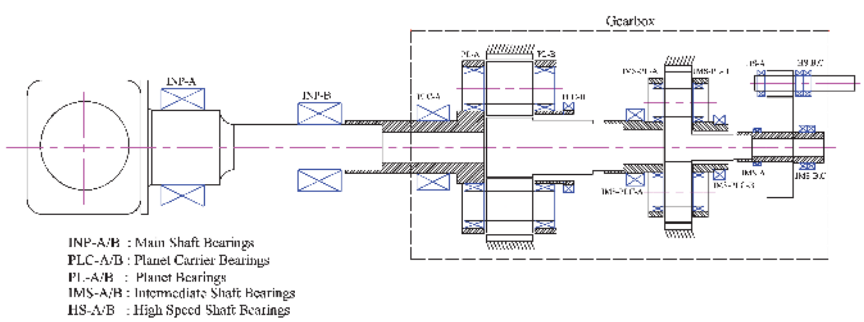

Figure 3. 5 MW reference gearbox schematic layout.

Table IV. 5 MW reference gearbox specification.

Parameter	Value
Type	2 Planetary + 1 Parallel
1st stage ratio	1:3.947
2nd stage ratio	1:6.167
3rd stage ratio	1:3.958
Total ratio	1:96.354
Designed power (kW)	5000
Rated input shaft speed (rpm)	12.1
Rated generator shaft speed (rpm)	1165.9
Rated input shaft torque (kN.m)	3946
Rated generator shaft torque (kN.m)	40.953
Total dry mass ($\times$1000 kg)	53
Service life (year)	20

DOI: 10.1002/we
Prepared using weauth.cls

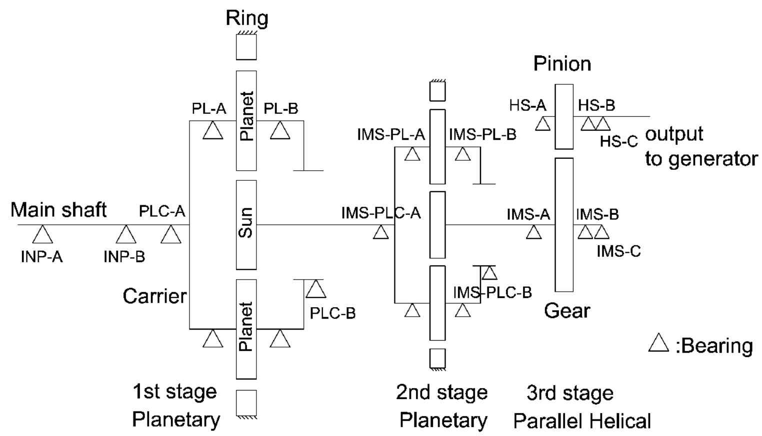

Figure 4. 5 MW gearbox topology.

3.1. Component Specifications

Table V presents the detailed geometrical specifications of gears in each stage. The bearing types and sizes are also shown in Table VI. In this reference gearbox, the sun gears, planets and parallel helical gears are case hardened-carburized steel and ring gears are quenched-tempered. All gears are made of 16MnCr5 with average core hardness of 25 HRC (Rockwell hardness scale).

Table V. Geometrical specification of gears.

Parameter	1^{st} stage	2^{nd} stage	3^{rd} stage
Type	Planetary	Planetary	Parallel
Ratio	1:3.947	1:6.167	1:3.958
Number of planets	3	3	-
Normal module (mm)	45	21	14
Normal pressure angle (degree)	20	20	20
Helix angle (degree)	0	0	10
Face width (mm)	491	550	360
Centre distance (mm)	863	584	861
Number of teeth, Sun/Pinion	19	18	24
Number of teeth, Planet/Gear	17	36	95
Number of teeth, Ring gear	56	93	-
Profile shift coefficient, Sun/Pinion	0.617	0.389	0.480
Profile shift coefficient, Planet/Gear	0.802	0.504	0.669
Profile shift coefficient, Ring gear	-0.501	0.117	-
Pitch diameter (mm), Sun/Pinion	855.000	378.000	341.183
Pitch diameter (mm), Planet/Gear	765.000	756.000	1350.517
Pitch diameter (mm), Ring gear	2520.000	1953.000	-
Tip diameter (mm), Sun/Pinion	978.839	432.845	380.751
Tip diameter (mm), Planet/Gear	905.440	815.655	1395.372
Tip diameter (mm), Ring gear	2475.087	1906.074	-
Root diameter (mm), Sun/Pinion	798.061	341.845	319.627
Root diameter (mm), Planet/Gear	724.662	724.655	1334.248
Root diameter (mm), Ring gear	2677.507	2000.574	-

Table VI. Geometrical specification of bearings.

Name	Type	OD	ID	B
INP-A	CARB	1750	1250	375
INP-B	SRB	1220	750	365
PLC-A	CRB	1030	710	315
PLC-B	SRB	1220	1000	128
PL-A	CRB	600	400	272
PL-B	CRB	600	400	272
IMS-PLC-A	CARB	1030	710	236
IMS-PLC-B	SRB	870	600	155
IMS-PL-A	CRB	520	380	140
IMS-PL-B	CRB	520	380	140
IMS-A	CRB	500	400	100
IMS-B	TRB	550	410	86
IMS-C	TRB	550	410	86
HS-A	CRB	360	200	98
HS-B	TRB	460	200	100
HS-C	TRB	460	200	100

OD/ID: outer/inner diameter, B: thickness. All dimensions are in mm. Types are as per SKF [53] terminology.

3.2. Gearbox Parameters for MBS Modelling

The MBS model of the 5 MW reference gearbox is shown in Fig. 5. The kinematic tree, presenting the interaction between each element body and their DOF are presented in Fig. 6 - see Fig. 4 for component names and topology.

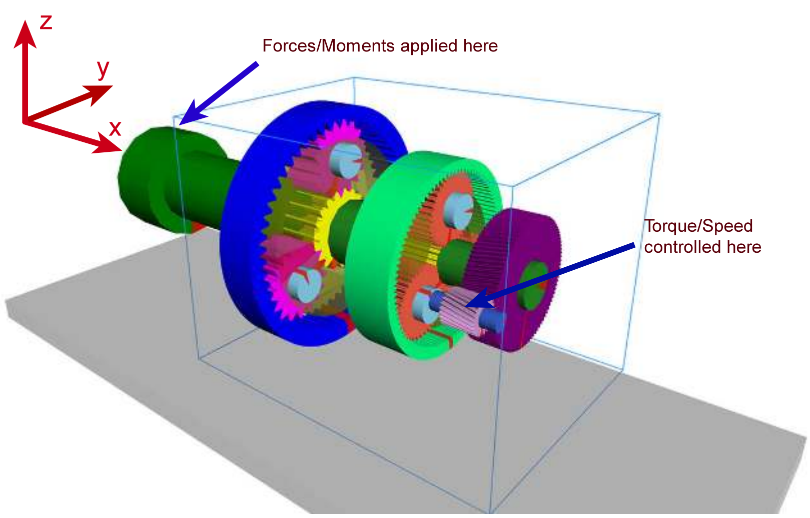

Figure 5. 5 MW gearbox MBS model.

The parameters required for MBS dynamic modelling (e.g. mass, inertia and stiffness) are listed in Table VII, VIII for gears and shafts and in the Table IX for bearings. The values are based on the coordinate system shown in Fig. 5. The local coordinate is located at center point of each component.

The eigenvalues and eigen modes of the gearbox according to the locations of nodes is listed in Table X.

The $I_{Gearbox}$ in 1-DOF torsional model - see section 2.6 - calculated from MBS model is 545900 $kg.m^2$ and with the torsional eigenfrequncy of 8.2 Hz, the $K_{Gearbox}$ is estimated to be about $1.5{\times}10^9$ Nm/rad.

4. GEARBOX VULNERABILITY MAP

A comprehensive design should include recommendations and comments on the maintenance planning and procedures. In Nejad et. al [10] a procedure to develop an inspection and maintenance planning map based on the fatigue damage of gears

Wind Energ. 0000; **00**:1–17 © 0000 John Wiley & Sons, Ltd.
DOI: 10.1002/we
Prepared using weauth.cls

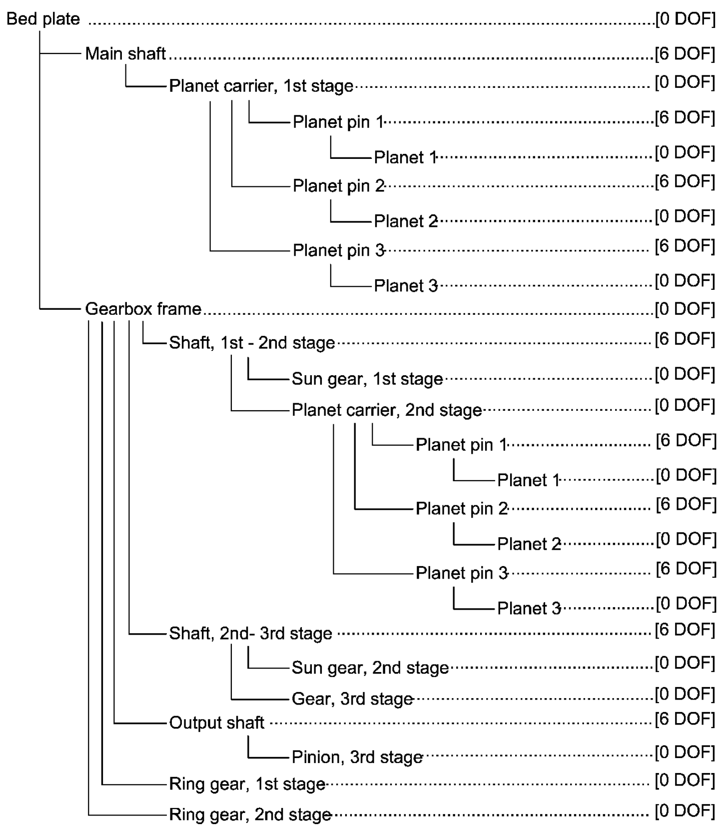

Figure 6. 5 MW gearbox MBS model kinematic tree.

Table VII. Dynamic model parameters of gears.

Parameter	Component	1^{st} stage	2^{nd} stage	3^{rd} stage
Mass(kg)	Sun/Pinion	1900	380	180
	Planet/Gear	1500	1500	1800
	Ring Gear	6000	3500	-
	Planet Carrier	5800	2100	-
I_{xx}(kg.m^2)	Sun/Pinion	244	9.5	3.8
	Planet/Gear	168	143	475
	Ring Gear	11900	3800	-
	Planet Carrier	4180	820	-
I_{yy}(kg.m^2)	Sun/Pinion	161	14	3.8
	Planet/Gear	115	110	260
	Ring Gear	6100	1990	-
	Planet Carrier	2200	450	-
I_{zz}(kg.m^2)	Sun/Pinion	161	14	3.8
	Planet/Gear	115	110	260
	Ring Gear	6100	1990	-
	Planet Carrier	2200	450	-
Mean gear contact stiffness (N/m)	-	9×10^9	1.5×10^{10}	7.5×10^9
Mean gear rotational stiffness (Nm/rad)	-	1.4×10^9	4.6×10^8	1.9×10^8

Table VIII. Dynamic model parameters of shafts.

Name	Mass($\times$1000 kg)	I_{xx}(kg.m^2)	I_{yy}(kg.m^2)	I_{zz}(kg.m^2)
Main Shaft	18	2180	14500	14500
1^{st}stage-2^{nd} Shaft	2.8	215	240	240
2^{nd}stage-3^{rd} Shaft	1.5	44	145	145
Output Shaft	0.2	1	7	7
Planet Pin, 1^{st}stage	0.7	15	49	49
Planet Pin, 2^{nd}stage	0.7	12	43	43

Table IX. Dynamic model parameters of bearings.

Name	K_x(N/m)	K_y(N/m)	K_z(N/m)	K_β(Nm/rad)	K_γ(Nm/rad)
INP-A	0	1.5×10^{10}	1.5×10^{10}	5×10^{6}	5×10^{6}
INP-B	4.06×10^{8}	1.54×10^{10}	1.54×10^{10}	0	0
PLC-A	6.6×10^{4}	1.7×10^{9}	1.1×10^{9}	5.6×10^{5}	1.3×10^{5}
PLC-B	6.6×10^{7}	1.7×10^{9}	1.1×10^{9}	5.6×10^{5}	1.3×10^{5}
PL-A	9.1×10^{4}	9.4×10^{9}	3.2×10^{9}	1.4×10^{6}	4.5×10^{6}
PL-B	9.1×10^{4}	9.4×10^{9}	3.2×10^{9}	1.4×10^{6}	4.5×10^{6}
IMS-PLC-A	9.1×10^{4}	6×10^{7}	1.2×10^{9}	7.5×10^{4}	7.5×10^{4}
IMS-PLC-B	9.1×10^{7}	6×10^{7}	1.2×10^{9}	7.5×10^{4}	7.5×10^{4}
IMS-PL-A	9.1×10^{4}	6×10^{7}	1.2×10^{9}	7.5×10^{4}	7.5×10^{4}
IMS-PL-B	9.1×10^{4}	6×10^{7}	1.2×10^{9}	7.5×10^{4}	7.5×10^{4}
IMS-A	0	6×10^{7}	1.2×10^{9}	7.5×10^{4}	7.5×10^{4}
IMS-B	7.4×10^{7}	5×10^{8}	5×10^{8}	1.6×10^{6}	1.8×10^{6}
IMS-C	7.8×10^{7}	7.4×10^{8}	3.3×10^{8}	1.1×10^{6}	2.5×10^{6}
HS-A	1.3×10^{8}	8.2×10^{8}	8.2×10^{8}	1.7×10^{5}	1×10^{6}
HS-B	6.7×10^{7}	8×10^{8}	1.3×10^{8}	1.7×10^{5}	1×10^{6}
HS-C	8×10^{7}	1×10^{9}	7.3×10^{7}	1.7×10^{5}	1×10^{6}

Table X. 5 MW Reference Gearbox eigenfrequencies (Hz) and eigen modes.

No.	Eigenfrequeny (Hz)	Mode Shape	Location
1	0	Rigid body mode	-
2	1.4	x-Translational	1^{st}Planet
3	1.4	x-Translation	2^{nd}Planet
4	8.2	α-Rotational	Global
5	26.7	Rotational & Translational	Global

and bearings has been introduced. This map -named "gearbox vulnerability map [10]"- ranks the gearbox components with highest to lowest fatigue damage. During routine inspection and maintenance, the vulnerability map can be used to find the faulty component by inspecting those with highest probability of failure rather than examining all gears and bearings. Such maps can be used for fault detection during routine maintenance and can reduce the down time and efforts of maintenance team to identify the source of problem [10].

For this 5 MW reference gearbox, the vulnerability map has been constructed based on the procedures introduced by Nejad et. al [10] and is shown in Figure 7.

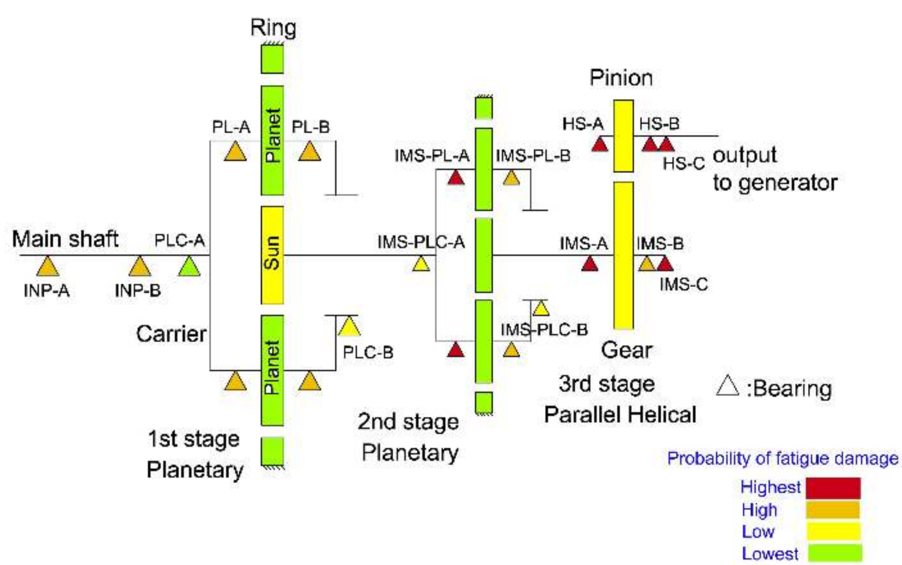

Figure 7. 5 MW gearbox vulnerability map.

Wind Energ. 0000; **00**:1–17 © 0000 John Wiley & Sons, Ltd.
DOI: 10.1002/we
Prepared using weauth.cls

5. SUMMARY & CONCLUDING REMARKS

In this paper, a 5 MW reference gearbox for offshore wind turbine is presented. The aim of this work is to support conceptual studies and design comparisons of various offshore wind turbines models. NREL 5 MW reference wind turbine has been broadly employed by researchers around the world for structural design studies, but currently, there is no gearbox model in wind turbine literatures for detailed investigations of drivetrains.

The system engineering approach has been employed for designing this reference gearbox. First, the gearbox weight is minimized by optimizing the gear speed ratios and then the components are designed. The 5 MW reference gearbox consists of three stages; two planetary and one parallel helical stage which is designed for the NREL 5 MW offshore reference wind turbine. The gearbox component design is based on the related international design codes and the data from similar type wind turbine gearboxes.

A multibody model of the gearbox is then developed. Gears are modelled as rigid bodies with compliance at tooth and bearings are represented with 6 DOF stiffness matrix. All parameters, including geometries, stiffness and topologies required for creating a dynamic model of the gearbox are provided. One can build this gearbox model in his own modelling tools and investigates the load and load response of different wind turbine designs in offshore developments.

ACKNOWLEDGEMENTS

The authors wish to acknowledge the financial support from Research Council of Norway through Norwegian Research Center for Offshore Wind Technology (Nowitech) and Center for Ships and Ocean Structures (CeSOS). The first author would like to thank Dr. K. Dykes from NREL for discussion on system engineering design approach.

REFERENCES

1. Jonkman J., Butterfield S., Musial W., and Scott G. Definition of a 5-mw reference wind turbine for offshore system development. Technical Report NREL/TP-500-38060, US National Renewable Energy Laboratory (NREL), 2009.
2. Cox K. and Echtermeyer A. Structural design and analysis of a 10mw wind turbine blade. *Energy Procedia*, 24:194–201, 2012.
3. Kaldellis J.K. and Zafirakis D.P. Trends, prospects and r & d directions in wind turbine technology. In Ali Sayigh, editor, *Comprehensive Renewable Energ*, pages 671–724. Elsevier, 2012.
4. Vestas. V112-3.3 mw offshore wind turbine. `www.vestas.com/en/products_and_services/turbines/`. [Online; accessed 03-April-2014].
5. Repower. Repower 5 mw wind turbine. `http://www.senvion.com/fileadmin/download/produkte/RE_PP_5M_uk.pdf/`. [Online; accessed 05-April-2014].
6. Areva. Areva m5000 wind turbine. `http://de.areva.com/EN/areva-wind-313/m5000-technical-data.html/`. [Online; accessed 07-April-2014].
7. Oyague F. Gearbox modelling and load simulation of a baseline 750-kw wind turbine using state-of-the-art simulation codes. Technical Report NREL/TP-500-41160, US National Renewable Energy Laboratory (NREL), 2009.
8. Dong W., Xing Y., Moan T., and Gao Z. Time domain-based gear contact fatigue analysis of a wind turbine drivetrain under dynamic conditions. *International Journal of Fatigue*, 48:133–146, 2013.
9. Dong W., Xing Y., and Moan T. Time domain modeling and analysis of dynamic gear contact force in a wind turbine gearbox with respect to fatigue assessment. *Energies*, 5:4350–4371, 2012.
10. Nejad A.R., Gao Z., and Moan T. Fatigue reliability-based inspection and maintenance planning of gearbox components in wind turbine drivetrains. *Energy Procedia*, 53:248–257, 2014.

11. Crowther A., Ramakrishnan V., Zaidi N. A., and Halse C. Sources of time-varying contact stress and misalignments in wind turbine planetary sets. *Wind Energy*, 14:637–651, 2011.
12. Xing Y., Karimirad M., and Moan T. Modelling and analysis of floating spar-type wind turbine drivetrain. *Wind Energy*, 17:565–587, 2014.
13. IEC 61400-1. Wind turbines, part 1: Design requirements, 2005.
14. Johannessen K., Meling T.S., and Haver S. Joint distribution for wind and waves in the northern north sea. *International Journal of Offshore and Polar Engineering*, 12(1):1–9, 2002.
15. K.O. Ronold and Gunner Chr. Larsen. *Variability of extreme flap loads during turbine operation*, pages 224–227. James and James Science Publishers, 1999.
16. IEC 61400-3. Wind turbines, part 3: Design requirements for offshore wind turbines, 2009.
17. Hawc2. Aero-servo-elastic calculation code for horizontal axis wind turbine, risoe centre, denmark technical university (dtu); denmark. `www.hawc2.dk/`. [Online; accessed 10-April-2014].
18. Nejad A.R., Jiang Z., Gao Z., and Moan T. Wind turbine gearboxes under blade pitch system fault, grid loss, and shut down events. submitted for publication, 2014.
19. Nejad A.R., Gao Z., and Moan T. On long-term fatigue damage and reliability analysis of gears under wind loads in offshore wind turbine drivetrains. *International Journal of Fatigue*, 61:116–128, 2014.
20. Nejad A.R., Gao Z., and Moan T. Long-term analysis of gear loads in fixed offshore wind turbines considering ultimate operational loadings. *Energy Procedia*, 35:187–197, 2013.
21. Nejad A.R., Xing Y., and T. Moan. Gear train internal dynamics in large offshore wind turbines. In *ASME 2012 11th Biennial Conference on Engineering Systems Design and Analysis*, pages 823–831. American Society of Mechanical Engineers, 2012.
22. Ning A. and Dykes K. Understanding the benefits and limitation of increasing maximum rotor tip speed for utility-scale wind turbines. In *The Science of Making Torque From Wind Conference Proceedings*, page in press, 2014.
23. Dykes K., Resor B., Platt A., Guo Y., Ning A., King R., Petch D., and Veers P. *Effect of tip speed constraints on the optimized design of a wind turbine*. National Renewable Energy Laboratory, in press, 2014.
24. AGMA. Ansi/agma/awea 6006-a03: standard for design and specifications of gearboxes for wind turbines. Technical report, AGMA, 2010.
25. ISO 6336-2. Calculation of load capacity of spur and helical gears, part 2: Calculation of surface durability (pitting), 2006.
26. AGMA. Agma information sheet: geometry factors for determing the pitting resistance and bending strength of spur, helical and herringbone gear teeth. Technical report, AGMA, 2000.
27. ISO 6336-3. Calculation of load capacity of spur and helical gears, part 3: Calculation of tooth bending strength, 2006.
28. IEC 61400-4. Wind turbines, part 4: Standard for design and specification of gearboxes, 2012.
29. D. W Dudley. *Handbook of Practical Gear Design*. McGraw-Hill Book Company, 1984.
30. R. J. Willis, Jr. New equations and charts pick off lightest-weight gears. *Product engineering*, pages 64–75, January 1963.
31. Eugene A. Avallone, Theodore Baumeister, and Ali M. Sadegh. *Mark's standard handbook for mechanical engineers*. McGraw-Hill Professional, 11th edition, 2006.
32. Robert Errichello. Notes on optimizing gearbox speed ratio. Technical report, NREL.
33. Orbital2. 2 mw variable speed gearbox. `http://www.orbital2.com/index.php/wind?showall=&start=6/`. [Online; accessed 03-April-2014].
34. Clipper Wind. 2.5 mw wind turbine. `http://www.clipperwind.com/product.htm/`. [Online; accessed 03-April-2014].
35. Nejad A.R., Xing Y., Guo Y., Keller J., Gao Z., and Moan T. Effect of floating sun gear in wind turbine planetary gearbox with geometrical imperfections. *Wind Energy*, accepted:in press, 2014.

DOI: 10.1002/we
Prepared using weauth.cls

36. ISO 6336-6. Calculation of load capacity of spur and helical gears, part 6: Calculation of service life under variable load, 2006.
37. KISSsoft. Design software for mechanical engineering applications. `http://www.kisssoft.ch/english/home/index.php/`. [Online; accessed 06-June-2014].
38. Repower. Repower 5 mw turbine technical data. `http://www.ceoe.udel.edu/windpower/resources/5m_uk.pdf`. [Online; accessed 05-April-2014].
39. Peeters J.L.M. *Simulation of dynamic drive train loads in a wind turbine*. Ph.D. thesis, Katholieke Universiteit Leuven, Belgium, 2006.
40. Ozguvent H.N. and Houser D.R. Mathematical models used in gear dynamics - a review. *Journal of sound and vibration*, 121(3):383–411, 1988.
41. Bauchau O.A. *Flexible multibody dynamics*. Springer, 2010.
42. Shabana A.A. *Dynamics of multibody systems*. Cambridge University press, 2013.
43. Xing Y. and Moan T. Multibody modelling and analysis of a planet carrier in a wind turbine gearbox. *Wind Energy*, 16(7):1067–1089, 2013.
44. Peeters J.L.M, Vandepitte D., and Sas P. Analysis of internal drive train dynamics in a wind turbine. *Wind Energy*, 9:141–161, 2006.
45. LaCava W., Xing Y., Guo Y., and Moan T. Determining wind turbine gearbox model complexity using measurement validation and cost comparison. *European Wind Energy Association annual event, Copenhagen*, 2012.
46. Guo Y., Keller J., Veers P., Sheng S., Austin J., Houser D., Nejad A.R., Xing Y., Gao Z., Moan T., Halse C., Crowther A., Errichello R., Helsen J., Bastard L., LaCava W., and McNiff B. *Gearbox reliability collaborative modelling round robin: gearbox system modelling practice*. National Renewable Energy Laboratory, in press, 2014.
47. SIMPACK. Multi body system software. `www.simpack.de/`. [Online; accessed 03-April-2014].
48. Calyx. a customizable multibody dynamic and static, 2d and 3d fe based contact solver engine. `http://ansol.us/Products/Calyx/`. [Online; accessed 05-June-2014].
49. Romax. Romaxwind software. `http://www.romaxtech.com/`. [Online; accessed 05-June-2014].
50. Kramer E. Dynamics of rotors and foundations, 1993.
51. Nakhaeinejad M. and Bryant M.D. Dynamic modeling of rolling element bearings with surface contact defects using bond graphs. *Journal of Tribology*, 133(1):011102, 2011.
52. Larsen T.J., Hansen M.H., and Iov F. *Generator dynamics in aerolastic analysis and simulations*. Riso National Laboratory, Riso-R-1395, 2003.
53. Skf bearings for wind turbines. `http://www.skf.com/group/industry-solutions/wind-energy/applications/gearbox/index.html/`. [Online; accessed 07-June-2014].